BP020-127N

Modelling the kinetics of enzymic reactions in mainly solid reaction mixtures

Peter J. Halling

Department of Pure and Applied Chemistry,
University of Strathclyde, 295 Cathedral Street,
Glasgow G1 1XL, United Kingdom

Stephen K. Wilson[1], Ralf Jacobs[2], Sean McKee and Christopher W. Coles

Department of Mathematics, University of Strathclyde,
Livingstone Tower, 26 Richmond Street,
Glasgow G1 1XH, United Kingdom

29th August 2002, revised 3rd February 2003

[1]Author for correspondence. Telephone: + 44 (0)141 548 3820, Fax: + 44 (0)141 552 8657, Email: s.k.wilson@strath.ac.uk

[2]Present Address: Lehrstuhl Allgemeine Elektrotechnik und Numerische Feldberechnung, Brandenburgische Technische Universität (BTU) Cottbus, Universitätsplatz 3-4, 03044 Cottbus, Germany

Abstract

There is currently considerable interest in using mainly solid reaction mixtures for enzymic catalysis. In these reactions starting materials dissolve into, and product materials crystalize out of, a small amount of liquid phase in which the catalytic reaction occurs. An initial mathematical model for mass transfer effects in such systems is constructed using some physically reasonable approximations. The model equations are solved numerically to determine how the reactant concentrations vary with time and position. In order to evaluate the extent to which mass transfer limits the overall rate of product formation an effectiveness factor is defined as the ratio of the observed total reaction rate to the total reaction rate in the reaction limited limit. As expected, the value of the effectiveness factor in steady state is strongly dependent on the Thiele modulus. However, it is also observed that the effectiveness factor can vary widely as a result of changes in the other dimensionless groups characterising the system. For example, there are situations with Thiele modulus equal to unity in which the value of the effectiveness factor varies between approximately 0.1 and 0.8 as the other parameters are varied in physically reasonable ranges. Analytical asymptotic solutions which provide good approximations to the numerically calculated results in various physically important limiting cases are also presented.

1 Introduction

There has recently been considerable interest in enzymic reactions taking place in mainly solid reaction mixtures (sometimes referred to as "solid-to-solid" reactions). In these reactions there is a small amount of liquid phase, often not immediately apparent, between the solid particles in which the catalytic reaction occurs. Starting materials dissolve from the solids into the liquid phase, and product materials are deposited from the liquid phase onto a different solid phase. As the reaction proceeds, the solid particles of the starting materials progressively shrink and disappear, while the product particles grow. These systems have considerable attractions for industrial applications, notably because of their very high reaction intensity (the final product level can exceed 900 g per kg of the reaction mixture, ten times higher than the usual maximum for a solution reaction). They can also combine high yields in reverse hydrolysis reactions (e.g. peptide synthesis) with good reaction rates, particularly when the liquid phase is aqueous. Further details about these reactions are given in the recent review articles by Erbeldinger et al. [1], Straathof et al. [2], and Ulijn et al. [3].

There has so far been only limited work on the kinetics of enzymic reactions in mainly solid reaction mixtures. Evidently mass transfer can be limiting since it only occurs by diffusion through the unstirred reacting mass. The full reaction-diffusion system is rather complicated. One or more starting materials diffuse from particles of the appropriate solid phase (usually crystals) to each point in the liquid phase. The product molecules diffuse in different directions towards the solid product particles (again usually crystals). Under mass transfer limited conditions, starting material and product concentrations will both vary considerably with position in the liquid phase, and with them the net reaction rate at that point. The problem is more complicated than any of the mass transfer reaction systems analysed in the context of immobilized enzymes (for example) because of the different directions of flux involved. As in the case of immobilized enzymes, the

use of enzymic catalysis is not relevant to the basic model. To the authors' knowledge, modelling of purely chemical reactions has not been attempted for this type of reaction system. This paper describes a first attempt to model the behaviour of such systems using idealised kinetics and a simple one-dimensional geometry. The resulting model predicts some expected features, but also some behaviour that is much harder to anticipate.

2 Model Formulation

The overall reaction involves the following processes.

(a) Dissolution of starting materials at the surface of the solid phase particles.

(b) Diffusion of the starting materials from the particle surfaces into all regions of the liquid phase.

(c) Enzyme-catalysed conversion to products.

(d) Nucleation of solid-phase product particles.

(e) Diffusion of product to the surface of the product particles.

(f) Growth of the product particles by attachment of new molecules.

All of the processes listed above take place in a more or less random network of solid particles with liquid filling the spaces in between them. Including all the details of the reaction would result in a very large and unwieldy model, and so in this initial study a number of approximations are employed in order to obtain a tractable model.

(a) Processes at the particle surfaces (dissolution, nucleation and growth) are disregarded. Even in stirred systems, solid dissolution or growth is commonly controlled by liquid phase mass transfer rather than surface processes (Grant and Higuchi [4]). In these unstirred reaction mixtures, mass transfer will be more likely to be rate

limiting, although there may be cases in which surface processes are important. (Indeed, there is experimental evidence that nucleation can limit overall kinetics in the early stages of an enzymic reaction in such systems, Erbeldinger et al. [5]).

(b) Related to (a), a system in which the product solid phase already exists and is simply growing with time by diffusion-controlled arrival of product molecules is considered.

(c) A reaction in which one starting material, denoted by A, is converted to one product, denoted by P, is considered. The majority of systems studied experimentally involve two starting materials. (They also involve a second product, but this is often water, which remains in the liquid phase.) Isomerisation reactions with only one starting material have been studied in mainly solid systems, such as the conversion of fructose to glucose investigated by Ulijn [6].

(d) The highly complicated real geometry is idealised to a liquid layer between two infinite parallel solid surfaces, one of starting material and the other of product. This reduces the problem to one in a single spatial dimension. The surfaces are considered as infinite sources and sinks. In reality the surfaces are actually free surfaces which change position as material dissolves or deposits, but the timescale of this movement will often be much greater than that for reaction and diffusion in the liquid layer. The net effect of this will be a slow translation of the entire liquid layer in the direction of the solid A, preserving all concentrations as a function of distance from the current positions of the solid surfaces. Furthermore, as the surfaces move, the liquid phase will remain of approximately constant thickness. Hence treating the solid boundaries as stationary (as we do here) is not unrealistic. Note that the layer thickness should not be interpreted simply as a typical distance between solid particles, but should be regarded as some sort of average distance between a liquid element and the nearest surfaces of the starting material and product particle.

(e) Both starting material and product are taken to have the same diffusion coefficient,

hereafter denoted by D, which is likely to be a good approximation (Green [7]).

(f) The reaction kinetics are described by the reversible Michaelis-Menten mechanism. This is usually a good approximation for one-substate enzymes under standard conditions (Fersht [8]). However, it can break down at high substrate and product concentrations such as those often found in mainly solid reaction mixtures. Nevertheless we adopt the Michaelis-Menten mechanism here because including additional physical effects (such as, for example, substrate inhibition) would significantly complicate the model. Note that the usual form of product inhibition, namely binding to the enzyme active site in competition with the substrate, is an integral part of the Michaelis-Menten mechanism.

The equation for the enzyme reaction rate ν (with dimensions of moles per unit volume per unit time) is written as

$$\nu(A,P) = \frac{\frac{V_{\max}}{K_{\mathrm{A}}}\left(A - \frac{P}{K}\right)}{1 + \frac{A}{K_{\mathrm{A}}} + \frac{P}{K_{\mathrm{P}}}} \tag{1}$$

where A and P are the concentrations of the starting material (substrate) and product respectively, K_{A} and K_{P} are the Michaelis constants for the enzyme (all of which have dimensions of moles per unit volume), K is the (dimensionless) chemical equilibrium constant, and $V_{\max}$ is the Michaelis-Menten maximum forward velocity (with dimensions of moles per unit volume per unit time). Hence we obtain the following reaction-diffusion equations that define the system,

$$\frac{\partial A}{\partial t} = D\frac{\partial^2 A}{\partial x^2} - \nu(A,P), \tag{2}$$

$$\frac{\partial P}{\partial t} = D\frac{\partial^2 P}{\partial x^2} + \nu(A,P), \tag{3}$$

for $0 < x < L$ and $t > 0$, subject to the boundary conditions

$$x = 0: \quad A = A^*, \quad \frac{\partial P}{\partial x} = 0, \tag{4}$$

$$x = L: \quad P = P^*, \quad \frac{\partial A}{\partial x} = 0, \tag{5}$$

and appropriate initial conditions. Here L is the thickness of the layer of liquid phase, and A^* and P^* are the saturated dissolved concentrations of the starting material A and product P, respectively.

The behaviour of the system is examined in the following three ways.

(a) Numerical integration of the full time evolution problem.

(b) Numerical integration of the steady state equations obtained by setting the time derivatives to zero.

(c) Analytical examination of various asymptotic limiting solutions of the steady state equations.

The details of the numerical method used are described in Appendix A, and analytical asymptotic solutions in various physically important limiting cases are presented in Appendix B.

The aims of the investigation are

(a) to identify how the reactant concentrations vary with position (and time), and

(b) to evaluate the extent to which mass transfer limits the overall rate of product formation.

In order to achieve (b), a dimensionless "effectiveness factor", hereafter denoted by E, is introduced by analogy with the classical treatment of immobilised enzyme kinetics. The quantity E is defined as the ratio of the observed total reaction rate to the total reaction rate in the reaction limited limit (i.e. the limit $D \to \infty$) in which the concentrations of A and P are equal to their saturation values of A^* and P^*, respectively, throughout the liquid reaction volume. As equation (1) shows, diffusional limitation (i.e. finite values of

D) will lead to concentrations $A < A^*$ and $P > P^*$, with correspondingly lower reaction rates. Hence E varies between unity in the reaction limited limit (i.e. the limit $D \to \infty$) to zero in the case of complete diffusional limitation (i.e. in the case $D = 0$). At steady state, the observed total rate per unit area may be evaluated as either

$$-D\frac{dA}{dx}\bigg|_{x=0} \quad \text{or} \quad -D\frac{dP}{dx}\bigg|_{x=L} \quad \text{or} \quad \int_0^L \nu(A,P)\,dx, \tag{6}$$

and so to obtain E this is divided by the total rate per unit area in the reaction limited limit, namely $\nu(A^*,P^*)L$, to yield

$$E = -\frac{DKK_{\mathrm{A}}\left(1+\dfrac{A^*}{K_{\mathrm{A}}}+\dfrac{P^*}{K_{\mathrm{P}}}\right)\dfrac{dP}{dx}\bigg|_{x=L}}{LV_{\max}(KA^*-P^*)}. \tag{7}$$

3 Dimensionless Model

The following five dimensionless groups were chosen to characterise the model.

(a) *The Thiele modulus* $\phi = (L^2V_{\max}/DK_{\mathrm{A}})^{1/2}$. This familiar dimensionless group represents a dimensionless measure of the relative importance of reaction and diffusion effects. It emerges naturally from the model equations, and its introduction eliminates any individual appearance of $V_{\max}$, L or D.

(b,c) *The ratios* A^*/K_{A} *and* P^*/K_{P}. These dimensionless ratios indicate the extent to which the enzyme is kinetically saturated with starting material A and product P at their saturating dissolved concentrations, respectively. These groupings emerge naturally from the model equations.

(d) *The chemical equilibrium constant* K. This parameter is dimensionless by definition, and was found to emerge as a key parameter in the asymptotic solutions.

(e) *The "solid equilibrium number"* $S = KA^*/P^*$. This dimensionless group is a measure of the thermodynamic driving force for the overall solid-to-solid conversion and

is by definition always greater than unity since a smaller value of S would correspond to a system in which "product" P was being converted to "starting material" A (in which case we could simply interchange the labels of A and P). The value of S can be estimated theoretically from the melting points of the reactants involved and a reference equilibrium constant for the class of reactions involved (Ulijn et al. [9]).

The system (1) – (5) is expressed in terms of the following dimensionless variables,

$$A' = \frac{A}{A^*}, \quad P' = \frac{P}{P^*}, \quad t' = \frac{V_{\max}}{K_{\mathrm{A}}} t, \quad x' = \frac{x}{L}, \quad \nu' = \frac{K_{\mathrm{A}}}{V_{\max} A^*} \nu, \tag{8}$$

in terms of which the reaction rate (1) can be written

$$\nu'(A', P') = \frac{A' - \frac{1}{S} P'}{1 + \frac{A^*}{K_{\mathrm{A}}} A' + \frac{P^*}{K_{\mathrm{P}}} P'}. \tag{9}$$

The equations (2) and (3) can be written

$$\frac{\partial A'}{\partial t'} = \frac{1}{\phi^2} \frac{\partial^2 A'}{\partial x'^2} - \nu'(A', P'), \tag{10}$$

$$\frac{K}{S} \frac{\partial P'}{\partial t'} = \frac{K}{\phi^2 S} \frac{\partial^2 P'}{\partial x'^2} + \nu'(A', P'), \tag{11}$$

for $0 < x' < 1$ and $t' > 0$, and are subject to the boundary conditions

$$x' = 0: \quad A' = 1, \quad \frac{\partial P'}{\partial x'} = 0, \tag{12}$$

$$x' = 1: \quad P' = 1, \quad \frac{\partial A'}{\partial x'} = 0, \tag{13}$$

and appropriate initial conditions. From equation (7) the effectiveness factor E is given by

$$E = -\frac{K}{\phi^2 (S-1)} \left(1 + \frac{A^*}{K_{\mathrm{A}}} + \frac{P^*}{K_{\mathrm{P}}}\right) \left.\frac{dP'}{dx'}\right|_{x'=1}. \tag{14}$$

4 Behaviour of the Model

4.1 Time Evolution of the Concentration Profiles Towards Steady State

Time evolutions of the concentration profiles of A and P for a variety of parameter values were obtained numerically using the method described in Appendix A. Initial conditions for these calculations were $A = A^*$ and $P = P^*$ for all $0 \leq x \leq L$ at $t = 0$, corresponding to the situation in which solid A and P are first equilibrated with the liquid phase and then the catalyst is rapidly mixed in to start the reaction. In all the cases investigated the concentrations were found to evolve fairly rapidly towards steady state values that were, in general, spatially non-uniform. Concentrations had normally reached within 1% of the final steady state values within a dimensionless time of about unity. Figure 1 shows a typical example of this evolution. In a typical reaction system, an enzyme with specific activity (i.e. activity per unit mass of enzyme) of 5 mol kg^{-1} s^{-1} (300 μmol mg^{-1} min^{-1}) might be present at a concentration of 2×10^{-4} kg l^{-1} (0.2 mg ml^{-1}), giving V_{max} of 10^{-3} mol l^{-1} s^{-1}. With K_A of 10^{-1} mol l^{-1} a dimensionless time of unity corresponds to 100 s, in contrast to a typical overall reaction time of several hours. So in this case concentrations are close to steady state over most of the reaction time, and hence the steady state solutions should provide a good picture of the physically relevant behaviour. It is, however, also possible to envisage parameter values such that unsteady conditions persist over much or all of the reaction. As well as being more complicated to model, behaviour will then be dependent on the initial profile of reactant concentrations, which are not easy to specify for most of the ways that reaction mixtures are prepared. Hence, in the remainder of the present paper we shall restrict our attention to the steady state solutions of the model. In particular, analytical asymptotic solutions for the steady state concentration profiles of A and P and the effectiveness factor E in the solid-to-solid equilibrium limit $S \to 1^+$, the reaction limited limit $\phi \to 0$, and the linear kinetics limit $A^*/K_A \to 0$ and $P^*/K_P \to 0$ are presented in Appendix B.

4.2 Steady State Concentration Profiles

The results of all the present numerical calculations indicate (although we have not formally proved) that provided that the initial concentration profiles $A(x,0)$ and $P(x,0)$ are monotonically decreasing functions of x then the concentration profiles $A(x,t)$ and $P(x,t)$ will remain monotonically decreasing for all $t > 0$, and hence, in particular, that the steady state concentration profiles will be monotonically decreasing.

Figure 2 shows two examples of the steady state concentration profiles of A and P for different values of K and S calculated numerically using the method described in Appendix A. Despite the fact that the Thiele modulus ϕ is equal to unity in both cases, the concentration profiles are evidently very different. In cases with little diffusional limitation such as that shown in figure 2(a), the steady state concentration profiles of both A and P remain close to their saturation values of A^* and P^*, respectively, throughout the liquid reaction volume. (Note the greatly magnified vertical scale in figure 2(a).) However, in other cases such as that shown in figure 2(b), diffusional limitation plays a significant role. In these cases A falls well below A^* away from the source of A at $x = 0$, and/or P rises well above P^* away from the sink of P at $x = L$. Note that figure 1 shows another example of this case in which P/P^* reaches large values away from $x = L$. Figure 2 also shows that, despite the fact that the values of $A^*/K_{\mathrm{A}} = 0.1$ and $P^*/K_{\mathrm{P}} = 0.1$ are not particularly small, in both cases the "exact" numerically calculated steady state concentration profiles are in excellent agreement with the corresponding asymptotic solutions in the linear kinetics limit $A^*/K_{\mathrm{A}} \to 0$ and $P^*/K_{\mathrm{P}} \to 0$ given in Appendix B. Note that in the first case (in which $S = 1.1$) the corresponding asymptotic solutions in the solid-to-solid equilibrium limit $S \to 1^+$, also given in Appendix B, are virtually identical to the asymptotic solutions shown in figure 2(a) and hence are omitted for clarity.

4.3 Values of the Effectiveness Factor

As described in section 2, we define the dimensionless effectiveness factor, E, as the ratio of the observed total reaction rate to the total reaction rate in the reaction limited limit in which the concentrations of A and P are equal to their saturation values of A^* and P^*, respectively. Values of E near unity indicate that reaction limitation dominates, while values near zero indicate that diffusional limitation dominates.

Figure 3 shows how the effectiveness factor E depends on the Thiele modulus ϕ in two different cases. As expected, in both cases shown E is close to unity for $\phi \ll 1$, and close to zero for $\phi \gg 1$. What is much less intuitively obvious is that when ϕ is of order unity, other parameters have a large effect on the value of E. The two cases shown are for relatively extreme parameter values, but clearly illustrate how in these cases the values of the other parameters can cause E to vary between approximately 0.1 and 0.8 when $\phi = 1$. Figures 1 and 2 also illustrate examples of situations with very different degrees of diffusional limitation when $\phi = 1$. Figure 3 also confirms that in both cases shown the numerically calculated values of E are in excellent agreement with the corresponding asymptotic values in the reaction limited limit ($\phi \to 0$) given in Appendix B provided that the value of ϕ is sufficiently small.

Figures 4 and 5 show the effects of the other parameters on the effectiveness factor E when $\phi = 1$. In particular, they show how E varies for parameter values in the following ranges, which were selected as those likely to describe real reaction systems for solid-to-solid conversions: A^*/K_A and P^*/K_P between 0.1 to 10, K between 0.1 and 100, and S between 1 and 1000.

Figure 4 shows E as a function of A^*/K_A for a range of values of P^*/K_P. In all the cases investigated, E was found to be a monotonically increasing function of A^*/K_A. Figure 4 also shows that (depending on the values of the other parameters) increasing the value of P^*/K_P can either increase or decrease E.

Figure 5 shows E as a function of the solid equilibrium number S for a range of values of K. In all the cases investigated, E was found to be a monotonically decreasing function of S, but a monotonically increasing function of K. Interestingly, there is no discontinuity in the behaviour of E as we approach $S = 1$, despite the fact that in this limit the net reaction rate becomes zero (the solid-to-solid conversion is at equilibrium). In particular, figure 5 shows how the numerically calculated values of E approach their appropriate limiting values given in Appendix B as S approaches unity.

5 Implications for Design of Reaction Systems

It is useful to briefly note how the dimensionless parameters may be altered in the design of a practical reaction system so as to achieve maximum effectiveness.

As in any mass transfer-reaction system, the Thiele modulus, $\phi = (L^2 V_{\max}/DK_{\mathrm{A}})^{1/2}$, should be minimised. The parameter $V_{\max}$ can always be reduced by lowering the catalyst concentration, but the penalty is of course a longer reaction time. The characteristic thickness of the layer of liquid phase L should be reduced by means of smaller reactant particles and more uniform mixing of them. The diffusion coefficient D will usually not change very much, but may be made smaller by using a solvent in which high reactant solubilities lead to a highly viscous liquid phase. The parameter A^*/K_{A} should be maximised. Both A^* and K_{A} can be changed by altering the solvent. However, they tend to vary by the same proportion, due to substrate solvation effects (van Tol et al. [10], Wescott and Klibanov [11], Janssen et al. [12]), in which case the ratio will be unchanged. More usefully, where more than one enzyme is available to catalyse the desired reaction, K_{A} may be reduced by selecting one with a higher affinity for the substrate. Changing K_{A} will, of course, also affect the value of ϕ, although only with a square root dependence. This will tend to have the opposite effect on E, and so the net result would need to be carefully determined in each individual case. The solid equilibrium number, $S = KA^*/P^*$, is a thermodynamic quantity that will be constant for a given reaction,

whatever the solvent. However, the chemical equilibrium constant K can be altered by changing the solvent, and the effectiveness factor, E, will be increased for larger K at any value of S. To increase K the chosen solvent should solvate P better than it does A. However, other factors are also important in the choice of solvent, and, in particular, it is often desirable to use just water. Solvent choice is also important for maximising equilibrium yield (Ulijn et al. [13]). Clearly, the possibilities for increasing effectiveness by changing these other parameters are somewhat limited. Nevertheless, it is evidently important to appreciate their effects in choosing a target value of ϕ to aim for in design.

6 Conclusions

An initial mathematical model for mass transfer effects in a mainly solid enzymic reaction mixture was constructed using some physically reasonable approximations. Numerically calculated solutions of the model equations show how reactant concentrations vary with time and position, and give an effectiveness factor E as a measure of the impact of mass transfer limitations. As expected, the value of E in steady state is strongly dependent on the Thiele modulus ϕ. However, it was also observed that E can vary widely as a result of changes in the other dimensionless groups characterising the system. For example, there are situations with $\phi = 1$ in which the value of E varies between approximately 0.1 and 0.8 as the other parameters are varied in physically reasonable ranges. Analytical asymptotic solutions which provide good approximations to the numerically calculated results in various physically important limiting cases were also presented. The relatively simple model discussed in this paper is based on a number of physically reasonable approximations and could, of course, be extended and improved in a variety of ways. Nevertheless we feel that the present results provide a useful insight into a highly complex physical system.

Acknowledgements

Professor Stephen Wilson acknowledges the financial support of the Leverhulme Trust via a Research Fellowship. Dr Ralf Jacobs wishes to acknowledge financial support from the European Consortium for Mathematics in Industry (ECMI) via the TMR Network Contract FMRX-CT97-0117 "Differential Equations in Industry and Commerce". All the authors gratefully acknowledge the preliminary numerical calculations undertaken by Dr Alain Gauthier, formerly in the Department of Mathematics, University of Strathclyde and currently in the Dipartimento di Mathematica, Politecnico di Milano, Milano, Italy. The authors also gratefully acknowledge valuable discussions with Dr Michael Grinfeld (Department of Mathematics, University of Strathclyde).

Appendix A: Details of the Numerical Method

In this appendix all quantities are dimensionless and so we omit the dashes for brevity.

In order to calculate the solution of the system (10)–(13) numerically the spatial domain $0 \leq x \leq 1$ and the temporal domain $t \geq 0$ were discretised using the finite difference grid $\{(j\Delta x, n\Delta t);\ j = 1, \ldots, M,\ n = 1, \ldots, N\}$ such that $M\Delta x = 1$ and $N\Delta t = T$ where T denotes the final time to be computed to. The numerically calculated values of A and P at $x = j\Delta x$ and $t = n\Delta t$ are denoted by A_j^n and P_j^n respectively.

After rearrangement, a full Crank-Nicolson discretisation of equations (10) and (11) results in

$$\begin{aligned} A_j^{n+1} - \frac{r}{2\phi^2}\delta_x^2 A_j^{n+1} + \frac{1}{2}\Delta t\left(\frac{A_j^{n+1} - P_j^{n+1}/S}{1 + A^* A_j^{n+1}/K_{\mathrm{A}} + P^* P_j^{n+1}/K_{\mathrm{P}}}\right) \\ = A_j^n + \frac{r}{2\phi^2}\delta_x^2 A_j^n - \frac{1}{2}\Delta t\left(\frac{A_j^n - P_j^n/S}{1 + A^* A_j^n/K_{\mathrm{A}} + P^* P_j^n/K_{\mathrm{P}}}\right), \end{aligned} \tag{15}$$

$$\begin{aligned} P_j^{n+1} - \frac{r}{2\phi^2}\delta_x^2 P_j^{n+1} - \frac{S}{2K}\Delta t\left(\frac{A_j^{n+1} - P_j^{n+1}/S}{1 + A^* A_j^{n+1}/K_{\mathrm{A}} + P^* P_j^{n+1}/K_{\mathrm{P}}}\right) \\ = P_j^n + \frac{r}{2\phi^2}\delta_x^2 P_j^n + \frac{S}{2K}\Delta t\left(\frac{A_j^n - P_j^n/S}{1 + A^* A_j^n/K_{\mathrm{A}} + P^* P_j^n/K_{\mathrm{P}}}\right), \end{aligned} \tag{16}$$

for $j = 1, \ldots, M$, where $r = \Delta t/(\Delta x)^2$ and δ_x^2 denotes the usual centered three-point finite difference approximation to a second spatial derivative.

The equations (15) and (16) may be written more compactly as

$$\mathbf{F}(\mathbf{z}^{n+1}) = \mathbf{b} \tag{17}$$

where $\mathbf{b}$ is a vector containing the previously calculated values A_j^n, P_j^n for $j = 1, \ldots, M$, and $\mathbf{z}^{n+1} = (\mathbf{A}^{n+1}, \mathbf{P}^{n+1})^T$ with $\mathbf{A}^{n+1} = (A_1^{n+1}, \ldots, A_M^{n+1})$ and $\mathbf{P}^{n+1} = (P_1^{n+1}, \ldots, P_M^{n+1})$. A (first order) discretisation of the boundary conditions (12) and (13) is incorporated into (17).

The algorithm consists of time-stepping forward using the Crank-Nicolson scheme (17). Since the equations are nonlinear the solution at each time step is obtained by using

several iterations of Newton's method, which may be written in the form

$$\mathbf{F}'(\mathbf{z}^n)(\mathbf{z}_{(i)}^{n+1} - \mathbf{z}_{(i-1)}^{n+1}) = -\mathbf{F}(\mathbf{z}^n) \tag{18}$$

where $\mathbf{F}'(\mathbf{z}^n)$ denotes the Jacobian

$$\left(\frac{\partial \mathbf{F}}{\partial \mathbf{z}}\right)_{\mathbf{z}=\mathbf{z}^n} \quad \text{or} \quad \left(\frac{\partial F_l}{\partial z_k}\right)_{z_k=z_k^n} \quad \text{for} \quad l,k = 1,\ldots,2M, \tag{19}$$

and $\mathbf{z}_{(i)}^{n+1}$ denotes the ith iteration of $\mathbf{z}^{n+1}$. A reasonable first guess for the Newton iteration is obtained by taking the value calculated at the previous time step, i.e. $\mathbf{z}_{(0)}^{n+1} = \mathbf{z}^n$.

The effectiveness factor E (calculated from the total rate per unit area) is then obtained by evaluating the integral

$$\int_0^1 \nu(A,P)\,dx \tag{20}$$

using the trapezoidal rule.

Appendix B: Steady State Asymptotic Solutions in Limiting Cases

In this appendix all quantities are dimensionless and so (as in Appendix A) we omit the dashes for brevity. Furthermore, we shall use the standard mathematical "order notation" in which $O(X)$ denotes terms of the same (or higher) order as X in the limit $X \to 0$.

From equations (10) and (11) in steady state A and P satisfy

$$\frac{1}{\phi^2}\frac{d^2A}{dx^2} = \frac{A - \frac{1}{S}P}{1 + \frac{A^*}{K_\mathrm{A}}A + \frac{P^*}{K_\mathrm{P}}P}, \tag{21}$$

$$\frac{K}{\phi^2 S}\frac{d^2P}{dx^2} = -\frac{A - \frac{1}{S}P}{1 + \frac{A^*}{K_\mathrm{A}}A + \frac{P^*}{K_\mathrm{P}}P}, \tag{22}$$

subject to the boundary conditions (12) at $x = 0$ and (13) at $x = 1$. Note that adding equations (21) and (22) and integrating twice yields $A + KP/S = \alpha x + \beta$ where α and β are arbitrary constants determined by imposing the boundary conditions.

B.1 The Solid-to-Solid Equilibrium Limit $S \to 1^+$

In the solid-to-solid equilibrium limit $S \to 1^+$ we have

$$A = 1 - \frac{K\left[1 + K\cosh C + Cx\sinh C - \cosh(Cx) - K\cosh(C(1-x))\right]}{2K + KC\sinh C + (1+K^2)\cosh C}(S-1) + O(S-1)^2, \tag{23}$$

$$P = 1 + \frac{K + \cosh C + KC(1-x)\sinh C - \cosh(Cx) - K\cosh(C(1-x))}{2K + KC\sinh C + (1+K^2)\cosh C}(S-1) + O(S-1)^2, \tag{24}$$

where we have defined

$$C = \phi\left[\frac{(1+K)}{K\left(1 + \frac{A^*}{K_\mathrm{A}} + \frac{P^*}{K_\mathrm{P}}\right)}\right]^{1/2}, \tag{25}$$

showing that, as expected, both A and P are equal to the constant value of unity at leading order, and that

$$E = \frac{(1+K)^2 \sinh C}{C\left[2K + KC\sinh C + (1+K^2)\cosh C\right]} + O(S-1). \tag{26}$$

Hence we find that at leading order E is a monotonically decreasing function of C satisfying $E = 1 - C^2/3 + O(C^4)$ as $C \to 0$, $E \sim (1+K)^2/KC^2 \to 0$ as $C \to \infty$, $E \sim 1/C \to 0$ as $K \to 0$ ($C \sim \phi(K(1 + A^*/K_\mathrm{A} + P^*/K_\mathrm{P}))^{-1/2} \to \infty$), and $E \sim \tanh C/C$ as $K \to \infty$ ($C \sim \phi(1 + A^*/K_\mathrm{A} + P^*/K_\mathrm{P})^{-1/2}$).

B.2 The Reaction Limited Limit $\phi \to 0$

In the reaction limited limit $\phi \to 0$ we have

$$A = 1 - \frac{(S-1)(2-x)x}{2S\left(1 + \dfrac{A^*}{K_\mathrm{A}} + \dfrac{P^*}{K_\mathrm{P}}\right)}\phi^2 + O(\phi^4), \tag{27}$$

$$P = 1 + \frac{(S-1)(1-x^2)}{2K\left(1 + \dfrac{A^*}{K_\mathrm{A}} + \dfrac{P^*}{K_\mathrm{P}}\right)}\phi^2 + O(\phi^4), \tag{28}$$

showing that, as expected, both A and P are equal to the constant value of unity at leading order, and that E is just less than unity and given by

$$E = 1 - \frac{\left[1 + K + \left(\dfrac{A^*}{SK_\mathrm{A}} + \dfrac{P^*}{K_\mathrm{P}}\right)(S+K)\right]}{3K\left(1 + \dfrac{A^*}{K_\mathrm{A}} + \dfrac{P^*}{K_\mathrm{P}}\right)^2}\phi^2 + O(\phi^4). \tag{29}$$

Note that it is necessary to calculate A and P to $O(\phi^4)$ (not shown here for brevity) in order to determine this $O(\phi^2)$ accurate expression for E.

B.3 The Linear Kinetics Limit $A^*/K_\mathrm{A} \to 0$ and $P^*/K_\mathrm{P} \to 0$

At leading order in the linear kinetics limit $A^*/K_\mathrm{A} \to 0$ and $P^*/K_\mathrm{P} \to 0$ equations (21) and (22) reduce to linear equations and so can be solved immediately to yield

$$A = \alpha x + \beta + c_+ \exp(cx) + c_- \exp(-cx) \tag{30}$$

and hence

$$P = S(\alpha x + \beta) - \frac{S}{K} c_+ \exp(cx) - \frac{S}{K} c_- \exp(-cx) \tag{31}$$

where the constants α, β, c_+ and c_- are given by

$$c_+ = \frac{K(S-1)(1+K\exp(-c))}{2S\left[2K + Kc\sinh c + (1+K^2)\cosh c\right]}, \tag{32}$$

$$c_- = \frac{K(S-1)(1+K\exp(c))}{2S\left[2K + Kc\sinh c + (1+K^2)\cosh c\right]}, \tag{33}$$

$$\alpha = -\frac{K(S-1)c\sinh c}{S\left[2K + Kc\sinh c + (1+K^2)\cosh c\right]}, \tag{34}$$

$$\beta = \frac{K(1+S) + KSc\sinh c + (K^2+S)\cosh c}{S\left[2K + Kc\sinh c + (1+K^2)\cosh c\right]}, \tag{35}$$

where we have defined

$$c = \phi\left[\frac{(1+K)}{K}\right]^{1/2}, \tag{36}$$

and hence

$$E = \frac{(1+K)^2\sinh c}{c\left[2K + Kc\sinh c + (1+K^2)\cosh c\right]}. \tag{37}$$

Hence we find that at leading order E is a monotonically decreasing function of c satisfying $E = 1 - c^2/3 + O(c^4)$ as $c \to 0$ and $E \sim (1+K)^2/Kc^2 \to 0$ as $c \to \infty$.

Clearly the solution in a number of interesting sublimits can be obtained from the solution in this limit. For example, in the solid-to-solid equilibrium limit $S \to 1^+$ we recover the appropriate special case of the results in section B.1 above, while in the limit $S \to \infty$ in which the solid-to-solid reaction is highly favourable we obtain

$$A \sim \frac{K + \cosh c + Kc(1-x)\sinh c + K\cosh(cx) + K^2\cosh(c(1-x))}{2K + Kc\sinh c + (1+K^2)\cosh c}, \tag{38}$$

$$P \sim \frac{S\left[K + \cosh c + Kc(1-x)\sinh c - \cosh(cx) - K\cosh(c(1-x))\right]}{2K + Kc\sinh c + (1+K^2)\cosh c}, \tag{39}$$

with E still given by (37). In the limit $K \to 0$ in which the liquid phase reaction is highly unfavourable then $c \sim \phi/\sqrt{K} \to \infty$ and we obtain

$$A \sim 1 - \frac{\phi(S-1)}{S} x\sqrt{K} + \frac{K(S-1)}{S}\left[K\exp(-cx) + \exp(-c(1-x))\right], \tag{40}$$

$$P \sim S - \phi(S-1)x\sqrt{K} - (S-1)\left[K\exp(-cx) + \exp(-c(1-x))\right], \tag{41}$$

and $E \sim \sqrt{K}/\phi \to 0$, showing that away from thin boundary layers of thickness $\sqrt{K} \ll 1$ near both $x = 0$ and $x = 1$ then both A and P are constant at leading order (with P being S times A, corresponding to the reaction being in equilibrium in the bulk of the liquid), while in the limit $K \to \infty$ in which the liquid phase reaction is highly favourable then $c \sim \phi$ and we obtain

$$A \sim \frac{\cosh\phi + (S-1)\cosh(\phi(1-x))}{S\cosh\phi}, \tag{42}$$

$$P \sim 1 + \frac{(S-1)\left[1 + (1-x)\phi\sinh\phi - \cosh(\phi(1-x))\right]}{K\cosh\phi}, \tag{43}$$

and $E \sim \tanh\phi/\phi$. In the reaction limited limit $\phi \to 0$ we recover the appropriate special case of the results in section B.2 above, while in the completely diffusion dominated limit $\phi \to \infty$ then $c \to \infty$ and we obtain

$$A \sim 1 - \frac{S-1}{S}x + \left(\frac{S-1}{Sc}\right)\left[K\exp(-cx) + \exp(-c(1-x))\right], \tag{44}$$

$$P \sim S - (S-1)x - \left(\frac{S-1}{Kc}\right)\left[K\exp(-cx) + \exp(-c(1-x))\right], \tag{45}$$

and $E \sim (1+K)/\phi^2 \to 0$, showing that away from thin boundary layers of thickness $1/c \ll 1$ near both $x = 0$ and $x = 1$ then both A and P are linear in x at leading order (with P being S times A, again corresponding to the reaction being in equilibrium in the bulk of the liquid).

References

[1] Erbeldinger, M.; Ni, X-W.; Halling, P.J. Enzymatic synthesis with mainly undissolved substrates at high concentrations. *Enzyme Microb. Technol.* **1998**, *23*, 141–148.

[2] Straathof, A.J.J.; Litjens, M.J.J.; Heijnen, J.J. Enzymatic transformations in suspensions. In *Methods in Biotechnology 15 - Enzymes in Nonaqueous Solvents*; Vulfson, E.N.; Halling, P.J.; Holland, H.L., Eds.; Humana Press: Totowa, New Jersey, 2001; pp 603–610.

[3] Ulijn, R.V.; De Martin, L.; Gardossi, L.; Halling, P.J. Biocatalysis in reaction mixtures with undissolved solid substrates and products. *Curr. Org. Chem.* **2002**, in press.

[4] Grant, D.J.W.; Higuchi, T. *Solubility Behaviour of Organic Compounds*; Wiley: New York, 1990; pp 474–541.

[5] Erbeldinger, M.; Ni, X-W.; Halling, P.J. Kinetics of enzymatic solid-to-solid peptide synthesis: inter-substrate compound, substrate ratio and mixing effects. *Biotechnol. Bioeng.* **1999**, *63*, 316–321.

[6] Ulijn, R.V. *Precipitation Driven Biocatalysis*; Ph.D. thesis, University of Strathclyde, Glasgow, 2001.

[7] Green, D.W. (Ed.) *Perry's Chemical Engineers Handbook*, 7th ed.; McGraw-Hill: New York, 1997; pp 5-50–5-54.

[8] Fersht, A. *Structure and Mechanism in Protein Science*; Freeman: New York, 1998; pp 104.

[9] Ulijn, R.V.; Janssen, A.E.M.; Moore, B.D.; Halling, P.J. Predicting when precipitation-driven synthesis is feasible: application to biocatalysis. *Chem. Eur. J.* **2001**, *7*, 2089–2098.

[10] van Tol, J.B.A.; Stevens, R.M.M.; Veldhuizen, W.J.; Jongejan, J.A.; Duine, J.A. Do organic solvents affect the catalytic properties of lipase? Intrinsic kinetic parameters of lipases in ester hydrolysis and formation in various organic solvents. *Biotechnol. Bioeng.* **1995**, *47*, 71–81.

[11] Wescott, C.R.; Klibanov, A.M. Thermodynamic analysis of solvent effect on substrate specificity of lyophilized enzymes suspended in organic media. *Biotechnol. Bioeng.* **1997**, *56*, 340–344.

[12] Janssen, A.E.M.; Sjursnes, B.J.; Vakurov, A.V.; Halling, P.J. Kinetics of lipase-catalysed esterification in organic media: correct model and solvent effects on parameters. *Enzyme Microb. Technol.* **1999**, *24*, 463–470.

[13] Ulijn, R.V.; De Martin, L.; Gardossi, L.; Janssen, A.E.M.; Moore, B.D.; Halling, P.J. Solvent selection for solid-to-solid synthesis. *Biotechnol. Bioeng.* **2002**, *80*, 509–515.

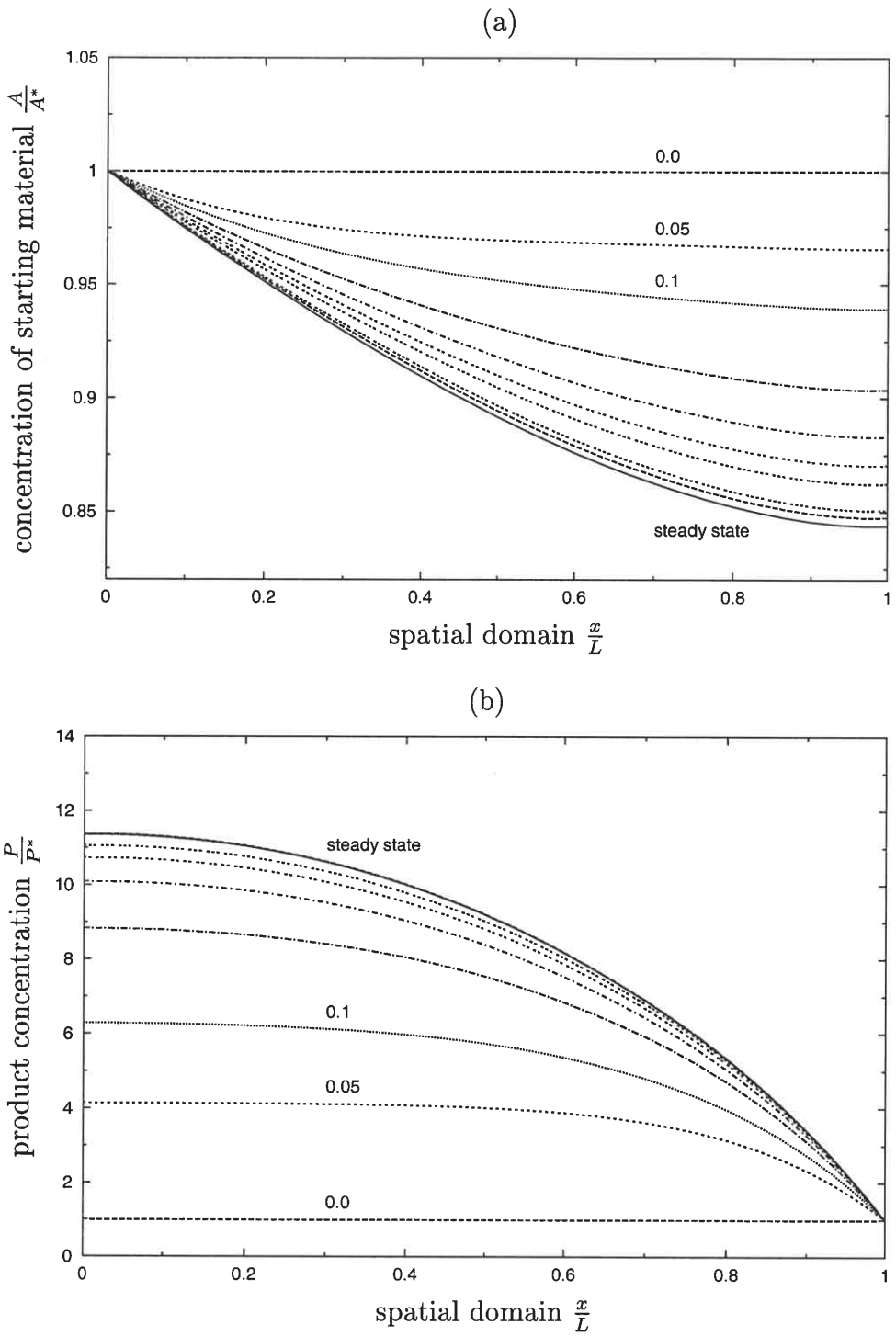

Figure 1: Time evolutions of the concentration profiles of (a) A/A^* and (b) P/P^* across the liquid reaction volume $0 \leq x/L \leq 1$ when $V_{\max}t/K_{\mathrm{A}} = 0.0, 0.05, 0.1, 0.2, 0.3, 0.4, 0.5, 0.8, 1.0$ and in steady state in the case $\phi = 1$, $A^*/K_{\mathrm{A}} = 0.1$, $P^*/K_{\mathrm{P}} = 0.1$, $K = 0.2$ and $S = 20$. Note the greatly magnified vertical scale in part (a), and that in part (b) the solutions when $V_{\max}t/K_{\mathrm{A}} = 0.8$ and 1.0 are virtually indistinguishable from the steady state solution.

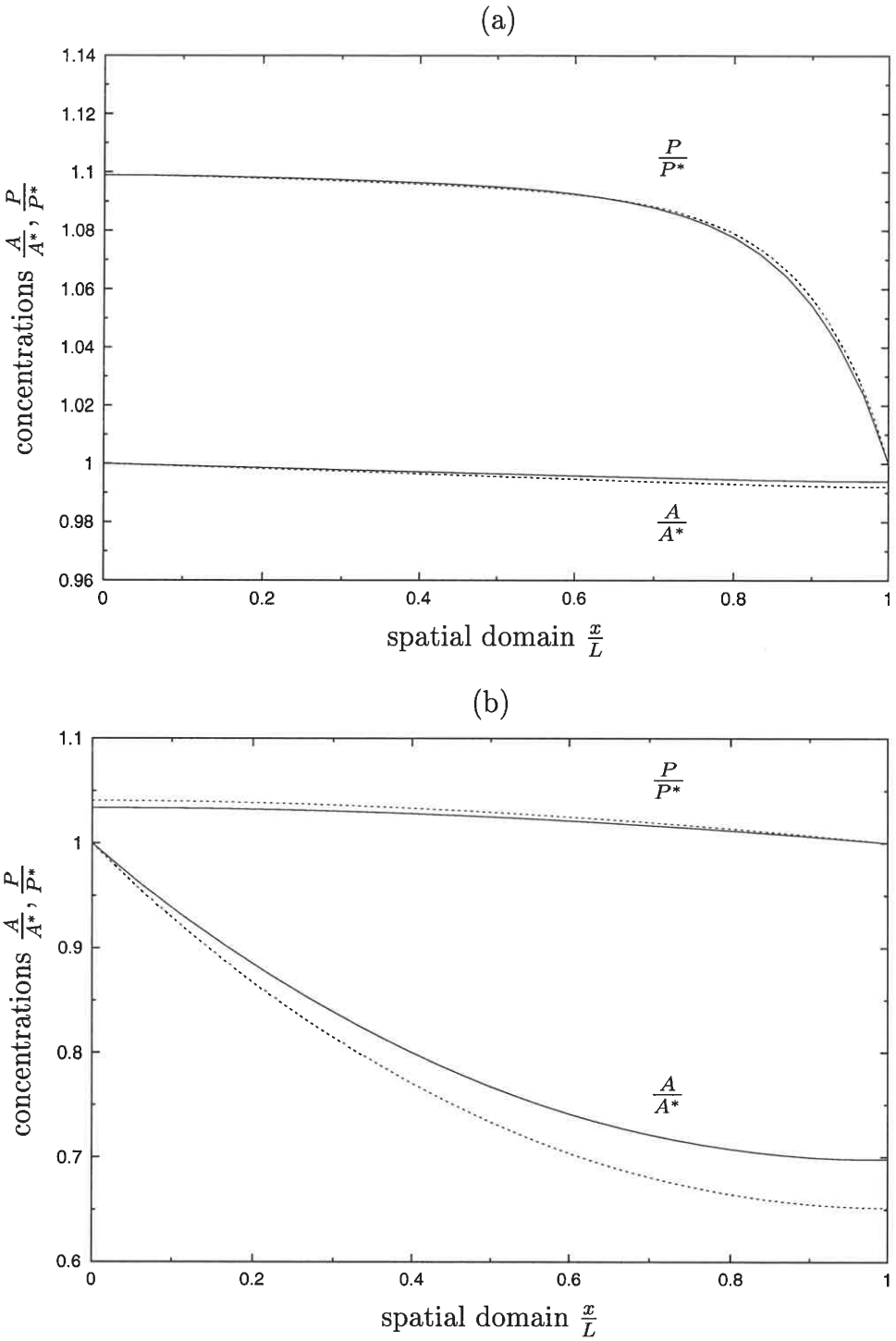

Figure 2: Examples of steady state concentration profiles when (a) $K = 0.011$ and $S = 1.1$, and (b) $K = 1000$ and $S = 100$ in the case $\phi = 1$, $A^*/K_A = 0.1$ and $P^*/K_P = 0.1$. The numerical results are denoted by solid lines and the corresponding asymptotic results in the linear kinetics limit ($A^*/K_A \to 0$ and $P^*/K_P \to 0$) given in section B.3 are denoted by dotted lines. Note the greatly magnified vertical scale in part (a).

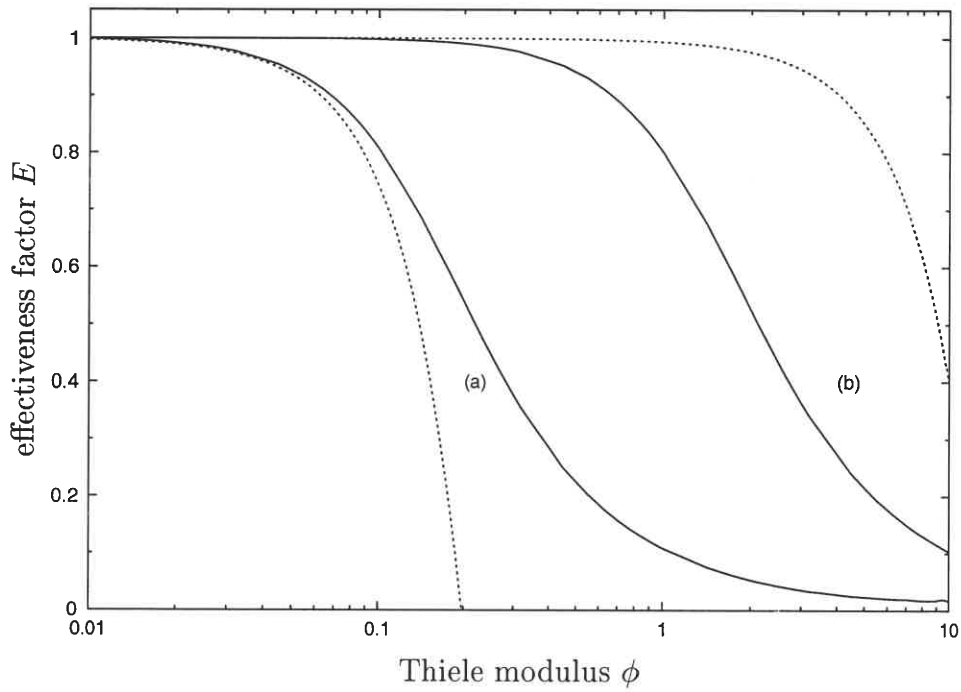

Figure 3: The effectiveness factor E plotted as a function of the Thiele modulus ϕ in the case $A^*/K_A = 0.1$, $P^*/K_P = 0.1$, $K = 0.011$ and $S = 1.1$ (case a), and the case $A^*/K_A = 10$, $P^*/K_P = 0.1$, $K = 100$ and $S = 10$ (case b). The numerical results are denoted by solid lines and the corresponding asymptotic results in the reaction limited limit ($\phi \to 0$) given in section B.2 are denoted by dotted lines.

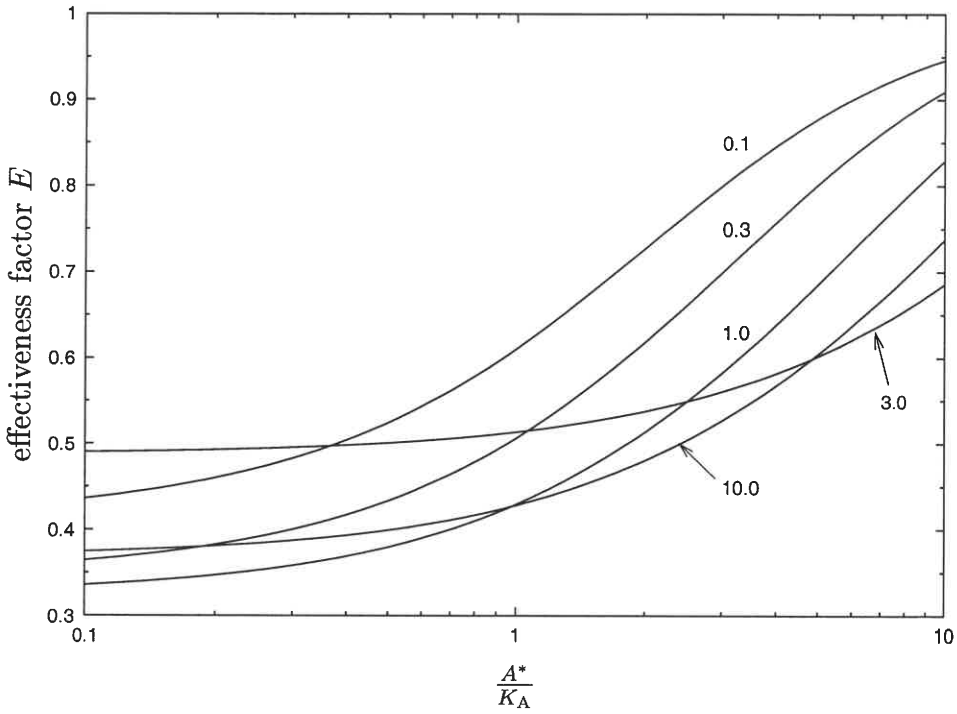

Figure 4: The effectiveness factor E plotted as a function of A^*/K_A for $P^*/K_P = 0.1$, 0.3, 1, 3 and 10 in the case $\phi = 1$, $K = 1$ and $S = 100$.

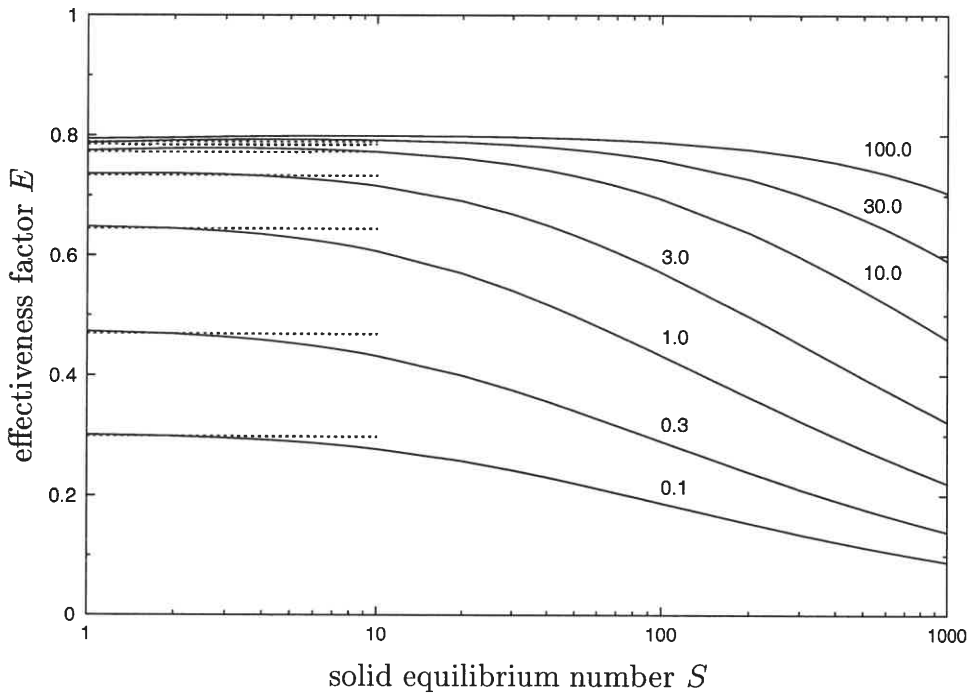

Figure 5: The effectiveness factor E plotted as a function of the solid equilibrium number S for $K = 0.1$, 0.3, 1, 3, 10, 30 and 100 in the case $\phi = 1$, $A^*/K_A = 0.1$ and $P^*/K_P = 0.1$. The dashed lines show the limiting values of E in the solid-to-solid equilibrium limit ($S \to 1^+$) given in section B.1.